

# Diameter-dependent voltammetric properties of carbon nanotubes

Chenguo Hu <sup>a,b</sup>, Yiyi Zhang <sup>c</sup>, Gang Bao <sup>c</sup>, Yuelan Zhang <sup>b</sup>,  
Meilin Liu <sup>b</sup>, Zhong Lin Wang <sup>b,d,\*</sup>

<sup>a</sup> Department of Applied Physics, Chongqing University, Chongqing 400044, China

<sup>b</sup> School of Materials Science and Engineering, Georgia Institute of Technology, Atlanta, GA 30332-0245, USA

<sup>c</sup> School of Biomedical Engineering, Georgia Institute of Technology and Emory University, Atlanta, GA 30332-0245, USA

<sup>d</sup> National Center of Nanoscience and Technology, Beijing, China

Received 22 September 2005; in final form 27 October 2005

Available online 1 December 2005

## Abstract

Voltammetric properties of electrodes made of multiple-walled carbon nanotubes (MWNTs) with different diameters were investigated by cyclic voltammetry. The results indicate that electrodes made of smaller MWNTs exhibit better voltammetric properties. In addition, electrodes made of mixed MWNTs with large diameter distribution possess the best voltammetric properties. The phenomenon can be explained by the filled-in frame structures formed on the electrode surface.

© 2005 Elsevier B.V. All rights reserved.

## 1. Introduction

Electrodes made using various carbon materials, such as glassy carbon, highly ordered pyrolytic graphite and boron-doped diamond are widely used in electrochemical applications [1–3]. Research has focused on understanding the factors that govern the electron transfer kinetics in carbon electrodes. The effect of solid carbon electrodes' surface structure in directing electron transfer reactions in electrochemistry has been well recognized, and the creation of specific surface structures, through pretreatments, such as plasma activation [4] and functional groups modification [5,6], can accelerate the electron transfer. The surface preparation and the final surface structure are often found to be critical to the performance of electrodes.

Due to their outstanding properties, carbon nanotubes (CNTs) are one of the most attractive nanomaterials in nanotechnology. Many potential applications of CNTs have been investigated, including electron field emitters [7], nanobalance [8], quantum resistors [9], nanoscale mass

conveyors [10], chemical sensors [11], rotational actuators [12], electronic biosensors [13], etc. Based on the specific surface structure of CNTs, applications in electroanalysis have also been studied, and most of them used CNTs to modify the surfaces of traditional electrodes, such as casting CNTs on Pt, Au [14] and glassy carbon electrodes [15], or intercalating MWNTs on graphite electrodes [16]. Some of these CNTs-modified electrodes failed to give well-resolved cyclic voltammograms [14], while others gave well-defined voltammetric responses [15] and can be used to detect low concentration biomolecules [16,17].

In this Letter, we present an alternative strategy by using CNTs film on inert glass substrate as the electrodes. The performance of CNTs electrodes was evaluated previously [18]. Since the diameters of nanotubes directly affect the microstructure on the surface of CNTs electrodes, here, we report the size-dependent voltammetric properties of CNTs electrodes. We found that electrodes made of nanotubes with smaller diameter exhibited better performance in voltammetric responses than that made of nanotubes with larger diameter. Besides, we found that electrodes made of nanotubes with mixed diameters exhibited the best voltammetric behaviors, and the voltammetric response was reversible.

\* Corresponding author. Fax: +1 404 894 9140.

E-mail address: [zhong.wang@mse.gatech.edu](mailto:zhong.wang@mse.gatech.edu) (Z.L. Wang).

## 2. Experiments

Multi-walled carbon nanotubes (MWNTs) with different diameters were purchased from Helix Material Solutions Inc. The nanotubes were dispersed and functionalized by following protocol. First, 2 mg MWNTs was mixed with 40 ml Tween 20 (1% in water) and sonicated for 30 min in a water-bath sonicator. Then the mixture was centrifuged for 10 min at 2000 rpm and 30 ml upper supernatant was collected carefully without disturbing the bottom part (10 ml). This step eliminated most big aggregates of MWNTs. The collected supernatant was then filtered with a disc membrane filter (pore size 200 nm) and the MWNTs pellet on the membrane was re-suspended in 4 ml water by brief sonication. The temperature of water bath was then adjusted to 55–58 °C and the MWNTs resuspension was continually sonicated while 2 ml nitric acid (15 M) was added drop by drop. After that the mixture was further sonicated for 20 min and then incubated at 45 °C for 4 h under shaking. After incubation, MWNTs was collected again by filtering and washed with copious water to remove nitric acid and other oxidized impurities. Glass slides (0.6 × 1 cm) were cleaned by boiling in Piranha's solution (concentrated H<sub>2</sub>SO<sub>4</sub>: 30% H<sub>2</sub>O<sub>2</sub>, volume ratio 7:3) for 30 min and rinsed with copious water. Aqueous solution of MWNTs (0.4–0.6 mg/ml) was applied onto the glass slide and dried on a heat block (60 °C). This process was repeated

several times until the final thickness of the MWNTs film reached about 20 μm (measured by SEM from side view).

The electrochemical studies were carried out in a typical three-electrode cell, using 1 M KCl solution containing 10 mM Fe(CN)<sub>6</sub>. Cyclic voltammetric measurements were performed using the MWNTs as working electrodes, a platinum wire as counter electrode and a SCE as a reference electrode. The data were recorded with an EG&G 273A Potentiostat/Galvanostat interfaced with a computer. All of the reagents are of analytic purity as supplied by Sigma–Aldrich, and deionized water obtained from a Millipore water system was used throughout. All electrochemical experiments were performed at room temperature (~23 °C).

## 3. Results and discussion

### 3.1. Characterization of the diameter of MWNTs and morphology of the electrodes

We prepared a set of electrodes with MWNTs of different diameters. Based on Fig. 1a, diameters of MWNTs range from 3 to 10, 10 to 20, 20 to 40 and 3 to 100 nm for electrodes 1#, 2#, 3# and A#, respectively. Diameter distributions were shown in Fig. 1b. The length of all the MWNTs ranged from 0.5 to 4 μm.

The surface morphology of these MWNTs electrodes were shown in Fig. 2 and the zoomed images are shown

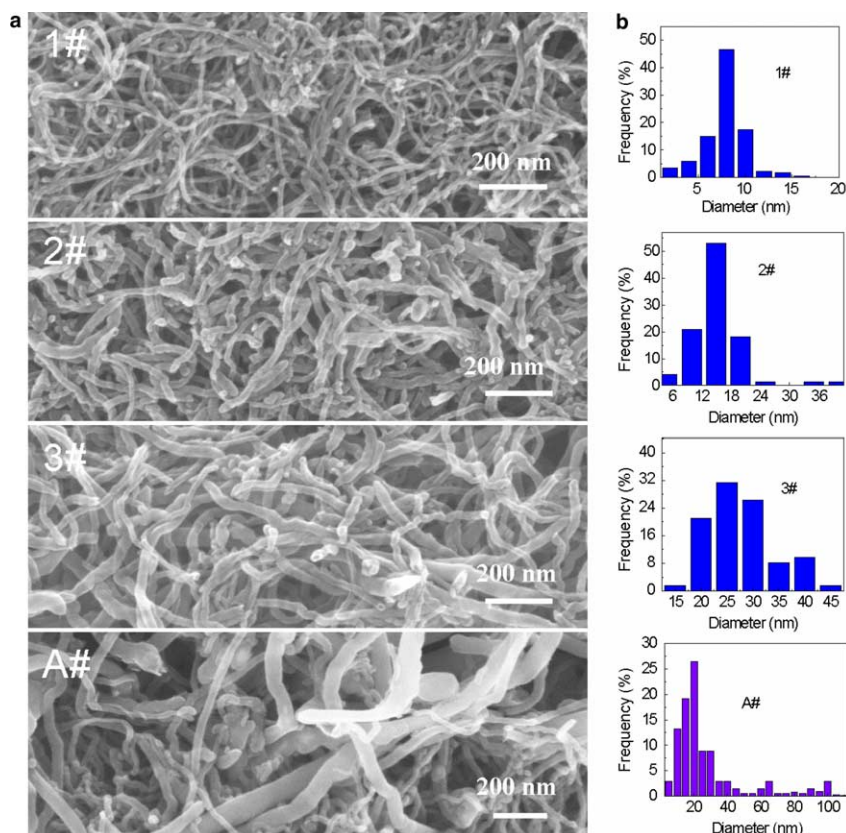


Fig. 1. (a) SEM images of the MWNTs electrodes and (b) the statistical diameter distributions by counting nanotubes from TEM images, indicating diameters of MWNTs range from 3 to 10, 10 to 20, 20 to 40 and 3 to 100 nm for electrode 1#, 2#, 3# and A#, respectively.

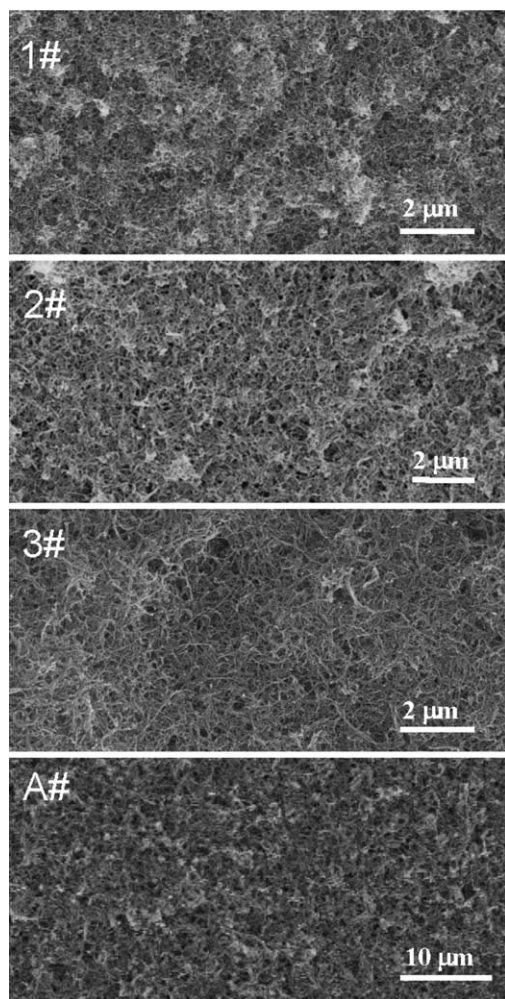


Fig. 2. Topography SEM images of the MWNTs electrodes, displaying uniform surfaces.

in Fig. 1a. All electrodes exhibited uniform surfaces with micro-pore structures. Such uniform films can only be obtained from well-dispersed nanotubes in solution phase.

### 3.2. Functional group and activation energy

We have reported that the voltammetric properties of MWNTs electrodes are mainly determined by quantity of active functional groups and activation energy of the electrodes [18]. A well-performing MWNTs electrode should have large quantity of carboxyl groups and low activation energy. To demonstrate presence of carboxyl groups on our nitric acid-treated MWNTs, FT-IR spectrum measurements were conducted. The results were shown in Fig. 3a. The peak at  $1725\text{ cm}^{-1}$  corresponds to C=O stretching vibration of carboxylic acids, while the peak at  $1390\text{ cm}^{-1}$  is associated with O–H bending deformation in carboxylic acids [19]. From this picture, we can also see that nanotubes with smaller diameter carry more functional groups, as indicated by the height of peaks at  $1725\text{ cm}^{-1}$ .

To determine the activation energy of each electrode sample, resistivity versus temperature plots were measured.

The results were shown in Fig. 3b. Based on our previously developed model [18],  $\rho = \rho_0 \exp\left(\frac{E_a}{kT}\right)$ , where  $\rho_0$  can be regarded as temperature-independent coefficient and  $E_a$  is activation energy, activation energy is calculated from the slope of the linearly fitting line in Fig. 4 and result is listed in Table 1.

### 3.3. Voltammetric properties in electrochemistry

Potential window is one of the most important factors for an electroanalytic electrode. A well-performing electrode can give high signal-to-noise ratio with flat and wide potential window. Fig. 4a indicates that the potential windows of the MWNTs electrodes are flat and wide in 0.1 M KCl. The redox reactions of potassium ferrocyanide usually serve as a benchmark in investigating electrochemistry at different carbon electrodes [20]. Here,  $\text{Fe}(\text{CN})_6^{4-}/\text{Fe}(\text{CN})_6^{3-}$  as redox pairs were used to investigate the influence of MWNTs diameter on the electronic transfer properties of the MWNTs electrode. The electrolyte was 1 M KCl throughout the work unless specially indicated. The diffusion rate of the reactant with the same concentration would be identical in spite of the difference of diameters among the testing MWNTs electrodes. So, the separation of redox peak potentials ( $\Delta E_p$ ) could directly correlate to the electron transfer rate. Shown in Fig. 4b are the cyclic voltammograms for MWNTs electrodes with different diameters. Each sample exhibits well-defined redox reactions with different peak potential separations, which are 98, 144, 150, 46 mV for sample 1#, 2#, 3# and A# at scan rate of  $20\text{ mV s}^{-1}$ , respectively. The behaviors of sample 1#, 2#, 3# electrodes implicated that the electron transfer rate at the electrode with smaller nanotube diameter is faster than that at the electrode with larger nanotube diameter. However, the electron transfer rate at the sample A#, with nanotube diameters range from 3 to 100 nm, is much faster than those at sample 1#, 2#, 3# and even faster than those at Pt and glass carbon electrode (the standard peak potential separation for reversible redox reactions is 59 mV at Pt electrode) [20].

Cyclic voltammograms at different scan rates were recorded to determine either the electron transfer rate or diffusion rate of the reactant is the rate-determining step. As shown in Fig. 4c, oxidation peak currents increase non-linearly with the increase of scan rate. Fitting the data in Fig. 4c resulted in the following equations (number), which showed that the peak currents at all these electrodes are proportional to the square root of the scan rate,

$$1\# : i_{\text{pa}} = -0.29 + 13.51v^{1/2}, \quad r = 0.999;$$

$$2\# : i_{\text{pa}} = -0.51 + 13.32v^{1/2}, \quad r = 0.999;$$

$$3\# : i_{\text{pa}} = -0.11 + 10.47v^{1/2}, \quad r = 0.999;$$

$$A\# : i_{\text{pa}} = -0.23 + 26.02v^{1/2}, \quad r = 0.994,$$

where  $i_{\text{pa}}$  and  $v$  is the oxidation peak current density in mA and scan rate in  $\text{V s}^{-1}$ , respectively. It indicates that diffu-

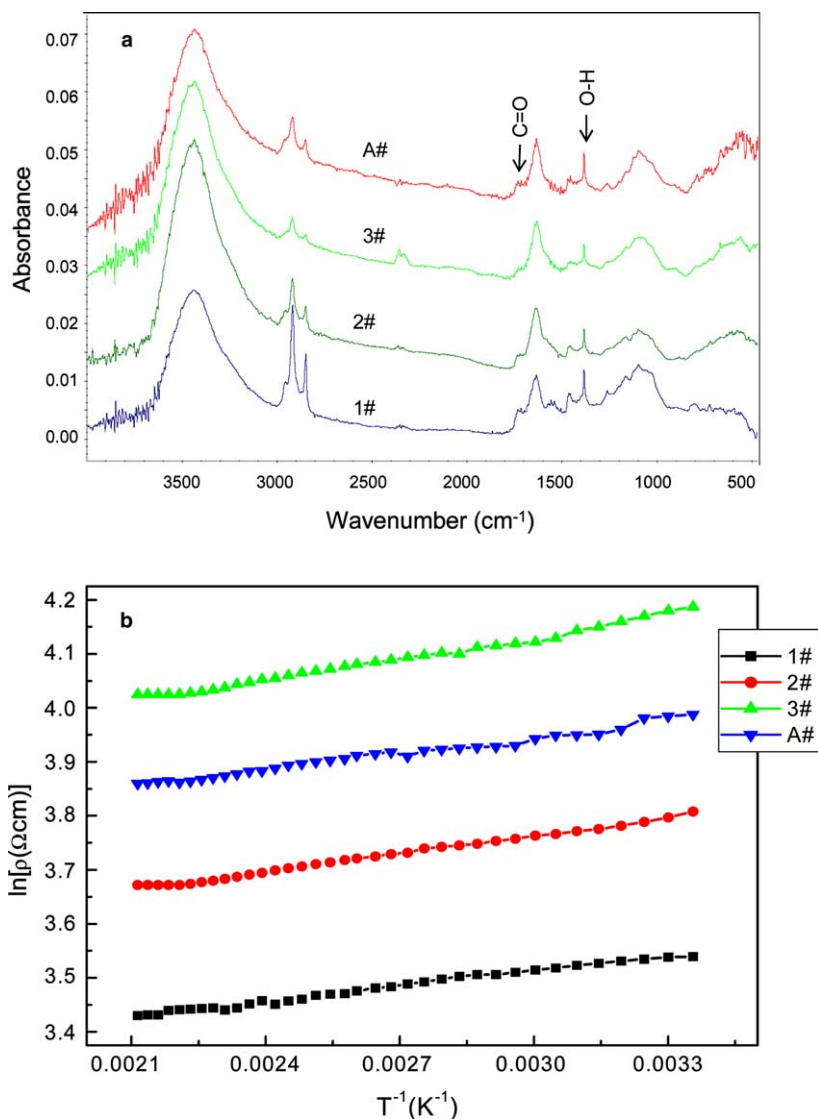


Fig. 3. (a) FT-IR spectra of the MWNTs from different samples, demonstrating the carboxyl groups binding on them and (b) the resistivity versus temperature plots for the MWNTs films.

sion rate of  $\text{Fe}(\text{CN})_6^{4-}$  limits the reaction rate in 1 M KCl. Hence, the electron transfer rate at the interface between electrode and solution is faster than diffusion rate of the reactant. A larger slope of lineally fitting line indicates a higher electron transfer rate. The above equations also indicated that sample A# showed the highest electron transfer rate among all samples.

Fig. 4d showed that the oxidation peak current densities increase lineally with  $\text{Fe}(\text{CN})_6$  concentration, which could be described with the following equations:

$$1\# : i_{\text{pa}} = 0.039 + 0.156C, \quad r = 0.997;$$

$$2\# : i_{\text{pa}} = 0.517 + 0.128C, \quad r = 0.997;$$

$$3\# : i_{\text{pa}} = 0.097 + 0.128C, \quad r = 0.997;$$

$$A\# : i_{\text{pa}} = 0.166 + 0.172C, \quad r = 0.995,$$

where  $i_{\text{pa}}$  and  $C$  is the oxidation peak current density in mA and concentration in mM, respectively. Since the large

slope corresponds to the low detection limit of the  $\text{Fe}(\text{CN})_6$ , the above equations demonstrates the MWNTs electrode with wide nanotube diameter distribution has the highest sensitivity in low reactant concentration.

Another advantage of the MWNTs electrodes is that there is no foul on the surface of the electrode because voltammograms are reproducible without any special pretreatment before each experiment except rinsing it with water. It is very important for MWNTs electrode to be used in electrochemical analysis, because the surface of bulk carbon electrodes usually become deactivated as a function of time when they are exposed to the laboratory atmosphere or working solution.

### 3.4. Discussion and analysis

The performances of the 3–10, 10–20 and 20–40 nm MWNTs electrodes indicated that the electrode of smaller

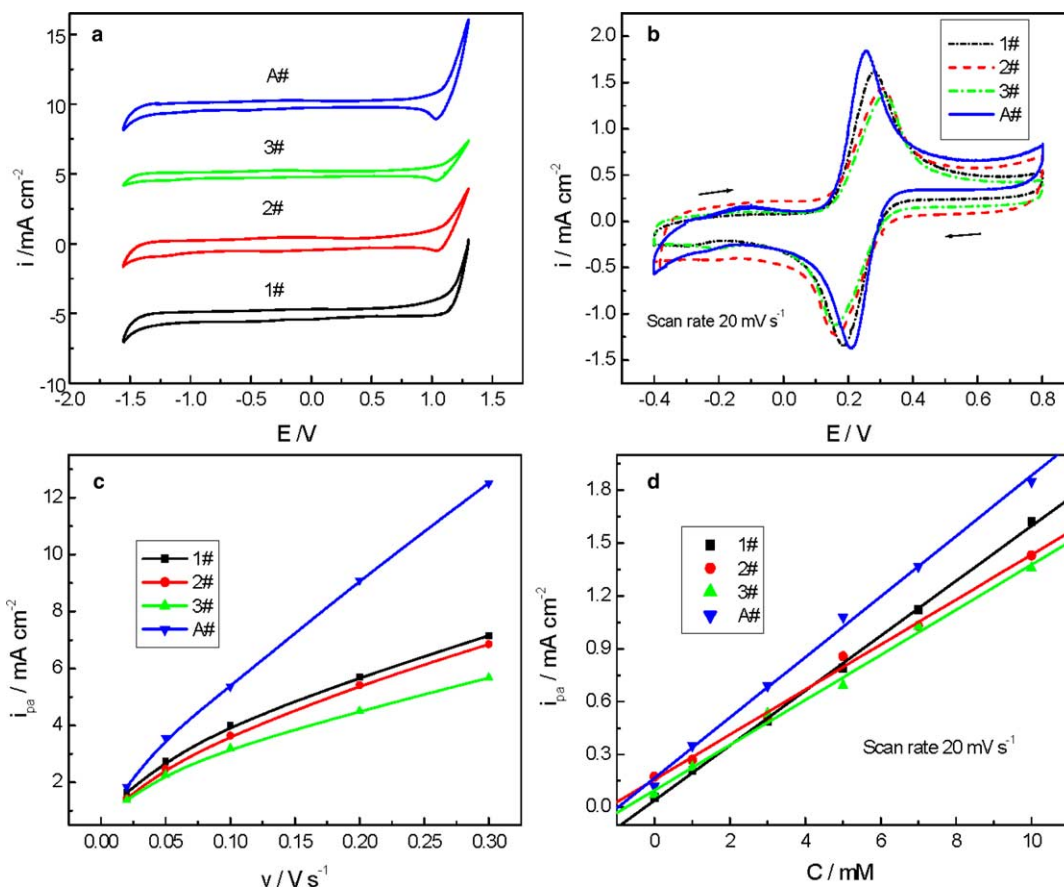


Fig. 4. Voltammetric behaviors of the MWNTs electrodes (a) potential window in 0.1 M KCl at scan rate of  $20 \text{ mV s}^{-1}$ , (b) cycle voltammogram for  $10 \text{ mM K}_4\text{Fe(CN)}_6$  in  $1 \text{ M KCl}$ , (c) the changes of oxidation peak current densities versus scan rate for  $10 \text{ mM K}_4\text{Fe(CN)}_6$  in  $1 \text{ M KCl}$  and (d) the changes of oxidation peak current densities versus concentration of  $\text{Fe(CN)}_6$  in  $1 \text{ M KCl}$ .

Table 1  
The activation energy of different electrode samples

	1#	2#	3#	A#
Activation energy (meV)	8.16	9.55	11.30	8.61

nanotube diameter distinguished itself in the detection sensitivity and electrode reaction kinetics from the other electrodes of larger nanotube diameter. This conclusion matches our previous model, because the electrode with smaller nanotube diameter shows higher peak of carboxyl group vibration in Fig. 3a and lower activation energy in Table 1. Take the 3–10 nm MWNTs electrode as an example; it has flat and wide potential window, faster electron transfer rate and lower concentration detection limit than those of 10–20 and 20–40 nm MWNTs electrodes. However, the voltammetric properties on the 3–100 nm MWNTs electrode is much better than those on the 3–10, 10–20 and 20–40 nm MWNTs electrodes. This result is beyond our expectation, since the number of carboxyl groups is not the largest and the activation energy is not the lowest on the 3–100 nm MWNTs electrode from Fig. 3a and Table 1. To explore the reason, we examined the surface of the electrode carefully and found out the special microstructure

on this electrode, as is shown in Fig. 5. The micro-pore surface is uniform in Fig. 5a and when the circle spot in Fig. 5a is enlarged, the frame structure displays that the thick nanotubes form skeleton of the frame from Fig. 5b. Then, when the circle spot in Fig. 5b is further enlarged, it shows lots of thin nanotubes fill in the frame from Fig. 5c. We make a sketch of such a structure in Fig. 5d. Such a filled-in frame structure is of three-dimensions and has higher surface to volume ratio than those of the electrode with narrow nanotube diameter distribution. Although the evidence of carboxyl group bond on the 3–100 nm nanotubes (Fig. 3a) and activation energy of the 3–100 nm MWNTs electrode (Table 1) is no better than that of 3–10 nm MWNTs electrode, it has higher surface to volume ratio as a result of its 3D filled-in frame structure than other electrodes, for which the electrode surface is much more than two-dimensional (Fig. 1a). It is the advantage of such structure that more functional groups can exert its effect in redox reactions. This result does not conflict our previous model. Though the activation energy is not the lowest among these four samples, but the number of functional groups involved in redox reactions should be the largest on the 3–100 nm MWNTs electrode due to its microstructure. So, it has best performance in voltammetric behaviors. From the analysis

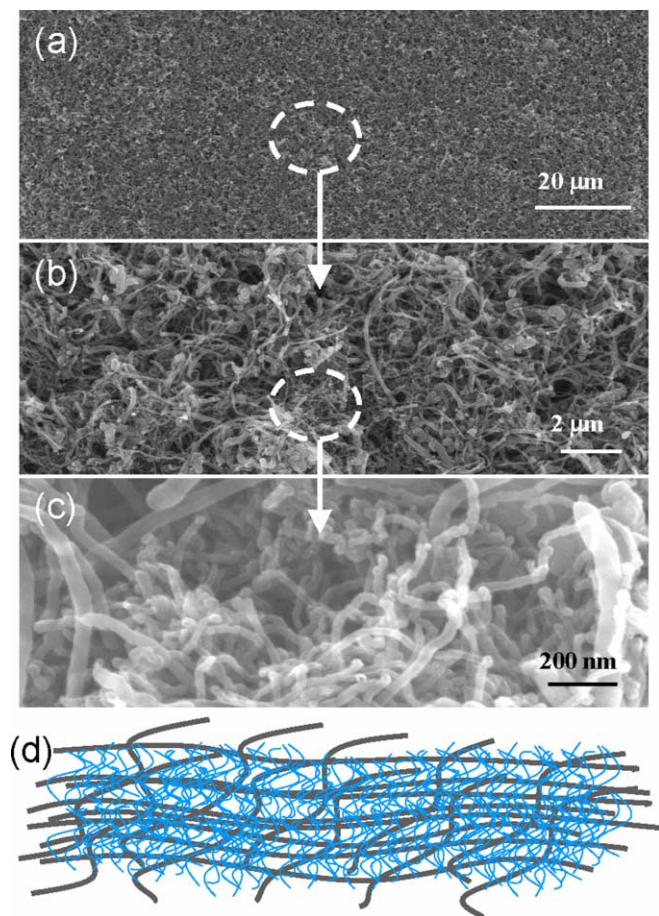


Fig. 5. SEM images of the surface of the 3–100 nm MWNTs electrode. (a) The uniform surface, (b) the image of enlarged circle spot in (a), exhibiting thick nanotubes forming the frame structure, (c) the image of enlarged circle area in (b), indicating the smaller nanotubes filling in the frame and (d) a schematic sketch of the filled-in frame structure on the surface of electrode.

above, it also demonstrates that availability of functional groups on the electrode for redox reaction plays key role in electroanalytic reaction.

#### 4. Conclusion

Voltammetric performance of the MWNTs electrodes can be enhanced by using MWNTs with smaller diameters. However, using MWNTs with wider diameter distribution can further enhance the performance of MWNTs elec-

trodes. Under this situation, MWNTs can form three-dimensional filled-in frame structures that possess higher surface to volume ratio and allows more functional groups to be involved in the redox reaction, hence facilitates surface-catalyzed reaction, which is proportional to surface coverage of functional groups.

#### Acknowledgments

This work is funded by National Nature Science Foundation of China (60376032), NSF and DARPA, Chinese Academy of Science.

#### References

- [1] K. Kinoshita, *Carbon: Electrochemical and Physicochemical Properties*, Wiley, New York, 1988.
- [2] J.P. Hart, M.J. Shearer, P.T. Mccarthy, S. Rahims, *Analyst* 109 (1984) 477.
- [3] J. Park, Y. Show, V. Quaiserova, J.J. Galligan, G.D. Fink, G.M. Swain, *J. Electroanal. Chem.* 583 (2005) 56.
- [4] J.F. Evans, T. Kuwana, *Anal. Chem.* 49 (1977) 1632.
- [5] P. Chen, R.L. McCreery, *Anal. Chem.* 68 (1996) 3958.
- [6] H. Yang, R.L. McCreery, *Anal. Chem.* 71 (1999) 4081.
- [7] W.A. de Heer, J.M. Bonard, K. Fauth, et al., *Adv. Mater.* 9 (1997) 87.
- [8] P. Poncharal, Z.L. Wang, D. Ugarte, W.A. de Heer, *Science* 283 (1999) 1513.
- [9] S. Frank, P. Poncharal, Z.L. Wang, W.A. de Heer, *Science* 280 (1998) 1744.
- [10] B.C. Regan, S. Aloni, R.O. Ritchie, U. Dahmen, A. Zettl, *Nature* 248 (2004) 924.
- [11] J. Kong, N.R. Frnklin, C.W. Zhou, M.G. Chapline, et al., *Science* 287 (2000) 622.
- [12] A.M. Fennimore, T.D. Yuzvinsky, W.Q. Han, M.S. Fuhrer, J. Cumings, A. Zettl, *Nature* 424 (2003) 408.
- [13] R.J. Chen, S. Bangsaruntip, K.A. Drouvalakis, N.W. Shi Kam, et al., *Appl. Phys. Sci.* 100 (2003) 4984.
- [14] C.Y. Liu, A.J. Bard, F. Wudl, I. Weitz, J.R. Heath, *Electrochem. Solid State Lett.* 2 (2001) 577.
- [15] H.X. Luo, Z.J. Shi, N.Q. Li, Z.N. Gu, Q.K. Zhuang, *Anal. Chem.* 73 (2001) 915.
- [16] Z.H. Wang, Q.L. Liang, Y.M. Wang, G.A. Luo, *J. Electroanal. Chem.* 540 (2003) 129.
- [17] A. Salimi, A. Noorbakhsh, M. Ghadermarz, *Anal. Biochem.* 344 (2005) 16.
- [18] C.G. Hu, W.L. Wang, K.J. Liao, et al., *J. Phys. Chem. Sol.* 65 (2004) 1731.
- [19] Y.H. Li, C. Xu, B.Q. Wei, *Chem. Mater.* 14 (2002) 483.
- [20] J. Bard, L.R. Faulkner, *Electrochemical Methods*, Wiley, New York, 2001.